Investigating UHPC in deck bulb-tee girder connections, part 1: Analytical investigation

Abdullah Haroon, Waleed Hamid, Eric Steinberg, Kenneth Walsh, Richard Miller, and Bahram Shahrooz

- An analytical study with ultra-high-performance concrete (UHPC) longitudinal joints was performed to investigate the joint performance when subjected to thermal and live loads.
- A continuity diaphragm with UHPC in the top flange was also investigated for negative moment over the pier.
- Results of the investigation suggest that the use of UHPC can improve the performance of the connections. The high bond strength of the UHPC reduces the connection length and allows for simpler reinforcement details.

Use of prefabricated bridge elements and systems helps achieve the objectives of accelerated bridge construction (ABC) by reducing on-site construction time and mobility impact time. Material quality, durability, and work-zone safety are also improved. For short to medium spans, precast, prestressed concrete voided core sections (adjacent box girders) are widely used for ABC; however, for spans of 100 ft (30 m) and above, the voided core sections become uneconomical and a precast, prestressed deck bulb-tee section is more suitable. Like voided core sections, the top flange of deck bulb-tee girders can act as the deck and eliminate the need for a cast-in-place concrete deck over the girders. A wider top flange of the deck bulb-tee girder results in an efficient prestressed section because many prestressing strands can be used before exceeding allowable stresses. The precast concrete top flange acting as a deck also allows for a variable deck thickness, which can result in a more efficient deck design. Despite the benefits of the deck bulb-tee bridge systems for ABC, their current use is limited to relatively short-span bridges with low traffic volume. The primary hurdle in the widespread adoption of these systems is concern related to the long-term performance of the connections between deck bulb-tee girders.

Previous longitudinal joint designs in deck bulb-tee bridge systems have been adequate for load transfer. However, frequent cracking of the longitudinal joints under service loading has been encountered.[1–4] These cracks often result in reflective cracking of any overlay material. The cracking

allows water and deicing chemicals to penetrate the joints, resulting in corrosion of reinforcing steel and deterioration of the girder concrete. Previous joint details used to connect the deck bulb-tee girders included a shear key with embedded angles field welded together using steel plates at a spacing of 4 ft (1.2 m) on center. This detail was sufficient in transferring shear; however, due to the longitudinal connectors being spaced at 4 ft, limited moment transfer occurred. This allows longitudinal flexural cracks to develop along the length of the joints. French et al.[5] developed and tested a revised detail that included continuous reinforcing bars embedded in the deck and extending transversely into the joint. The joint reinforcement consisted of extended deck reinforcement in a U-shaped hoop. This detail, when used with high-strength concrete, showed improved flexural resistance; however, small cracks still developed at service-level loads.

The transverse joint (continuity joint) between deck bulb-tee girders is typically made using a cast-in-place concrete diaphragm connecting the girders over the pier; however, this requires a large transverse joint to fully develop the continuity reinforcement. Also, conventional cast-in-place concrete results in a joint section that has less strength and durability than the rest of the girder.

Using ultra-high-performance concrete (UHPC) as all or a portion of the closure placement material in deck bulb-tee bridge systems can address the joint issues. UHPC has improved compressive and tensile strengths compared with conventional concrete, excellent bonding properties, and superior durability. Field-cast UHPC joints have performed better and are more durable than the conventional concrete joints.[6] The high bond strength between UHPC and reinforcement requires shorter development lengths. This allows the girder connections to be smaller, and straight bar details can be used.

The research presented in this paper is the analytical portion of a larger study performed under National Cooperative Highway Research Program project 18-18. The analytical findings guided the direction of a full-scale experimental testing program, which will be the subject of a companion paper. To enable the wider adoption of deck bulb-tee systems for medium- to large-span bridges, UHPC is investigated as an alternative to conventional concrete to provide the required strength and durability for the longitudinal joints between flanges and transverse joints between girders. Design guidelines and standard details must be developed for UHPC joints in deck bulb-tee systems to ensure adequate performance of the joints and allow for accelerated construction. Variables that need to be considered include connection width, bar spacing, bar size, bar detailing (straight, bent, or headed), flange thickness, and closure placement material. The use of UHPC as closure placement material can be a viable option to increase the durability of the joints. The high bond strength of UHPC allows shorter development lengths that allow for simpler bar detailing in the joints.

Analytical program

A comprehensive analytical program with the following objectives was performed:

- Determine longitudinal connection design for UHPC deck bulb-tee girders.
- Perform parametric analyses on longitudinal joint design to assess effects of span, skew, and girder depth on the joint.
- Investigate effects of thermal loading and live loading on the longitudinal joint.
- Evaluate transverse joint design using partial-depth UHPC for continuity.

Stage 1

The primary purpose of the stage 1 analytical modeling was to design bridges representative of the actual deck bulb-tee girder systems. A total of 27 five-girder bridge models (labeled case 1 to case 27) were developed that varied in girder section, span length, concrete unit weight, skew, and cross slope. The girders were designed based on the ninth edition of the American Association of State Highway and Transportation Officials' *AASHTO LRFD Bridge Design Specification* under HL-93 live loading and self-weight. No other loading was considered (for example, barriers, braking, wind, or earthquakes) in this stage. Commercial bridge design software was used to check whether the bridges were practical. The girder designs from these models were used in stage 2 and stage 3, where detailed modeling of the connections using UHPC was performed and investigated for live and thermal loadings.

The girder section was dependent on the design requirements, such as the span and girder spacing. The precast concrete economical fabrication (PCEF) deck bulb-tee section was used as a starting point because the experimental testing eventually used this section. The other primary sections available are the Precast/Prestressed Concrete Institute Northeast (PCINE) and Washington State Department of Transportation (WSDOT) wide flange deck bulb tee. All three sections have differences in basic geometry. Both the PCINE and WSDOT sections have options for 60 or 96 in. (1.5 or 2.4 m) wide flanges. WSDOT sections also come in 72 and 84 in. (1.8 and 2.1 m) flange widths. PCINE uses an 8 in. (200 mm) thick flange, while the WSDOT girders can have a flange thickness as small as 6 in. (150 mm). Because the WSDOT girders can be deeper and have large flange widths and thin flanges, this section was used for select models.

The bridge models had four different span lengths of 55, 100, 150, and 200 ft (17, 30, 46, and 61 m). The span-to-depth ratios for the four span lengths were 16.9, 25.5, 28.6, and 23.3 respectively. Although 55 ft is a short span for the deck bulb-tee system, it was used to match the span of the girders

used for the full-scale experimental testing during phase 2 of this study. The larger spans were also considered because they required a deeper deck bulb-tee and this could affect behavior of the joint because taller webs with the same web thickness are a less rigid support for the flanges. In addition, the longer spans may have larger camber, which could affect differential camber considerations.

The shorter-span bridges do not require a deep deck bulb-tee section; therefore, lightweight concrete was not considered for spans of 55, 100, and 150 ft (17, 30, and 46 m); however, for spans of 200 ft (61 m), both normalweight and lightweight concrete were considered.

Most bridges have skews under 30 degrees. Therefore, different skews were investigated: 0 degrees, 15 degrees, and 30 degrees. The case with 0-degree skew was expected to have the simplest behavior. According to AASHTO LRFD specifications article 9.7.1.3, the primary reinforcement in the deck may be placed in the direction of the skew if the skew angle does not exceed 25 degrees. Reinforcement in the joint, and hence primary reinforcement in the flanges, was placed perpendicular to the web to meet AASHTO requirements; however, skew cases required fanning of the reinforcement near the ends.

The cross slope on deck bulb-tee girder bridges can be obtained in various ways. An overlay can be added with varying thickness, the girders can be set with their webs out of plumb, or the deck bulb-tee flanges can be sloped to achieve the cross slope. Most cross slopes do not exceed 2%, and therefore this was investigated using the methods of placing the girders 2% out of plumb and sloping the deck bulb-tee flanges 2%.

Table 1 provides a summary of the sections considered along with the number of 0.6 in. (15 mm) Grade 270 (1860 MPa) low-relaxation strands necessary for the exterior and interior girders. The exterior girders often required more strands due to their higher distribution factors. The girder section used for cases 1 through 18 was PCEF and for cases 19 through 27 was WSDOT. Cases 1 through 22 were modeled as normalweight concrete, whereas cases 23 through 27 were modeled as lightweight concrete.

Distribution factors The live load distribution factors (LLDFs) provided by the AASHTO LRFD specifications[7] for the decked precast, prestressed concrete bulb tees are based on type j, which is specific for the precast, prestressed concrete tee section with shear keys and with or without transverse post-tensioning. This case assumes that the bridge is "sufficiently connected to act as a unit." It was assumed that the use of a UHPC joint was sufficient to interconnect the elements of a deck bulb-tee system, and therefore, type j was used to calculate the distribution factors. Part of the stage 3 finite element method (FEM) modeling was to verify the distribution factors.

Table 1 provides the distribution factors for the design cases considered. The exterior girders have higher distribution factors than the interior girders, which often occurs in design under the AASHTO LRFD specifications. The fairly large differences in the moment distribution factors for the exterior and interior deck bulb-tee girders may lead to exterior girders having up to eight additional strands. Designers often design the interior girders the same as the exterior controlling girder because of ease of constructibility. If the exterior girder is designed differently from the interior girder, excessive differences may occur in camber between interior and the exterior girders, leading to further difficulties during construction.

Deck and longitudinal joint design The design of the top flange, which serves as the deck for the deck bulb-tee bridge system, was important to the research because it provides the transverse reinforcement for the longitudinal joint between girders. AASHTO LRFD specifications article 5.12.2.3.3b notes that decks with flexural-shear joints should be modeled as continuous plates and the empirical design procedure of article 9.7.2 should not be used. Therefore, the deck, which was the upper flange of the deck bulb-tee section, was designed using the strip method. This required entering the deck bulb-tee sections with an upper flange that consisted of only the nonprismatic section and using the thinner portion of the upper flange as the thickness of the deck. The longitudinal deck reinforcement for all bridge models consisted of no. 5 (16M) bars at 16 in. (410 mm) spacing at the top and no. 6 (19M) bars at 12 in. (300 mm) spacing at the bottom. The transverse reinforcement of the deck was governed by the longitudinal joint reinforcement requirements and consisted of two layers of no. 5 bars spaced at 6 in. (150 mm).

Currently, there are no design specifications in the United States for UHPC. To date, the most helpful document for UHPC connection design is covered in Graybeal.[8] This document provides guidance related to cover, development length l_d, lap splice length l_s, and spacing of bars, along with associated commentary for the design of the UHPC connection details. **Table 2** summarizes these recommendations for no. 4, 5, and 6 (13M, 16M, and 19M) bars. Because no. 6 bars require a large embedment length, the width of the longitudinal joint would have to be increased. In addition, cover requirements increase for larger bars, which leave the bars less effective in flexure. Therefore, two layers of transverse no. 5 reinforcement protruded from the top flange of the deck bulb tee. The bars extended 5.5 in. (140 mm) into the joint. The transverse reinforcement was spaced at 6 in. (150 mm) in the girder and offset longitudinally in adjacent girders to create a 3 in. (75 mm) reinforcement spacing in the joint. The reinforcement in the joint was fanned at skewed ends to allow for placement without interference. **Figure 1** shows the detail of the longitudinal joint.

Continuity connection Due to the high cost of the UHPC, it was decided to provide the UHPC only in the upper portion of the diaphragm to resist the higher negative moment. The lower portion of the diaphragm would consist of the conventional concrete. The AASHTO LRFD speci-

Table 1. Stage 1 design parameters and moment LLDFs

Case	Span, ft	Flange width, in.	Flange thickness, in.	Section depth, in.	Skew, degrees	Girder	Interior/exterior 0.6 in. strands			AASHTO moment LLDFs			
										Interior girder		Exterior girder	
							Harped	Straight	Total	*+M*	*V*	*+M*	*V*
1	55	70.625	5.75	39	0	Plumb	2/2	10/10	12/12	0.813	0.813	0.656	0.698
2	55	70.625	5.75	39	15	Plumb	2/2	10/10	12/12	0.814	0.847	0.657	0.728
3	55	70.625	5.75	39	30	Plumb	2/2	10/10	12/12	0.772	0.886	0.625	0.761
4	55	70.625	5.75	39	0	2%	2/2	10/10	12/12	0.770	0.884	0.624	0.760
5	55	70.625	5.75	39	30	2%	2/2	10/10	12/12	0.770	0.884	0.624	0.760
6	55	70.625	2% slope*	39	0	Plumb	2/2	10/10	12/12	0.813	0.813	0.661	0.698
7	100	70.625	5.75	47	0	Plumb	4/4	18/22	22/26	0.814	0.814	0.580	0.699
8	100	70.625	5.75	47	15	Plumb	4/4	18/22	22/26	0.814	0.848	0.580	0.728
9	100	70.625	5.75	47	30	Plumb	4/4	18/22	22/26	0.785	0.887	0.560	0.762
10	100	70.625	5.75	47	0	2%	4/4	18/22	22/26	0.814	0.814	0.580	0.699
11	100	70.625	5.75	47	30	2%	4/4	18/22	22/26	0.785	0.887	0.560	0.762
12	100	70.625	2% slope*	47	0	Plumb	4/6	18/22	22/28	0.814	0.814	0.584	0.699
13	150	70.625	5.75	63	0	Plumb	10/10	24/32	34/42	0.814	0.814	0.555	0.699
14	150	70.625	5.75	63	15	Plumb	10/10	24/32	34/42	0.814	0.844	0.556	0.725
15	150	70.625	5.75	63	30	Plumb	10/10	24/32	34/42	0.788	0.879	0.538	0.755
16	150	70.625	5.75	63	0	2%	10/10	24/32	34/42	0.814	0.814	0.555	0.699
17	150	70.625	5.75	63	30	2%	10/10	24/32	34/42	0.788	0.879	0.538	0.755
18	150	70.625	2% slope*	63	0	Plumb	10/10	24/32	34/42	0.814	0.814	0.558	0.699
19	200	60	6	103	0	Plumb	10/16	32/32	42/48	0.814	0.814	0.569	0.699
20	200	96	6	103	0	Plumb	12/16	34/38	46/54	1.059	1.059	0.696	0.849
21	200	96	6	103	30	Plumb	12/16	34/38	46/54	1.017	1.123	0.669	0.901
22	200	60	2% slope*	103	0	Plumb	10/10	30/32	40/42	0.655	0.655	0.514	0.634
23	200	60	6	103	0	Plumb	10/10	24/28	34/38	0.814	0.814	0.569	0.699
24	200	60	6	103	30	Plumb	10/10	22/28	32/38	0.786	0.864	0.550	0.742
25	200	96	6	103	30	Plumb	10/12	26/32	36/44	1.017	1.123	0.669	0.901
26	200	96	6	103	0	Plumb	10/12	28/34	38/46	1.059	1.059	0.696	0.849
27	200	60	2% slope*	103	0	Plumb	10/12	28/34	38/46	1.059	1.059	0.882	0.882

Note: AASHTO = American Association of State Highway and Transportation Officials; LLDF = live-load distribution factor; *+M* = positive bending moment; PCEF = precast concrete economical fabrication; *V* = shear force; 1 in. = 25.4 mm; 1 ft = 0.305 m.

* The flanges of the girders were sloped to achieve bridge cross slope, but thickness remained constant.

fications requires the continuity diaphragm to be designed for both the negative moments over the pier due to applied loads and the positive restraint moments due to time-dependent effects. Because the UHPC was in the negative moment region, the continuity connection was investigated for negative moment design only.

To investigate the negative moment over the pier, four cases (cases 1, 7, 19, and 20) from simple-span design (Table 1) were extended to form bridge sections with two spans of equal length. Live loading due to an HL-93 truck was considered, and reinforcement area was determined based on Grade 60 (414 MPa) steel.

Table 2. Ultra-high-performance concrete connection design recommendations

Bar size	Criteria	Cover, in.	l_d, in.	l_s, in.	Spacing, in.
No. 4	UHPC	≥1.5	4.0	3.0	≤3.0
		≥1.0 but <1.5	5.0	3.75	≤3.75
No. 5	UHPC	≥1.875	5.0	3.75	≤3.75
		≥1.25 but <1.875	6.25	4.69	≤4.69
No. 6	UHPC	≥2.25	6.0	4.50	≤4.5
		≥1.5 but <2.25	7.5	5.63	≤5.63

Note: l_d = development length; l_s = lap splice length; UHPC = ultra-high-performance concrete. No. 4 = 13M; no. 5 = 16M; no. 6 = 19M.

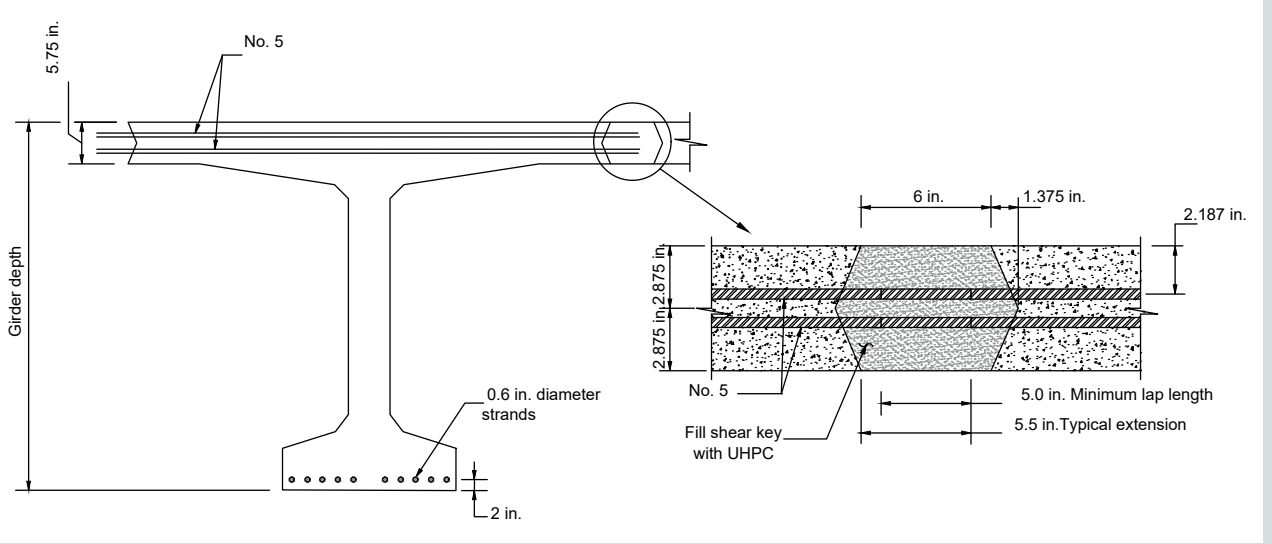

Figure 1. Girder longitudinal keyway detail. Note: H = girder depth; UHPC = ultra-high-performance concrete. No. 5 = 16M; 1 in. = 25.4 mm.

Table 3. Continuity joint reinforcement for negative moment

Case	Spans, ft	$-M_u$, kip-ft	Required A_s, in.^{2}	Diaphragm width b, in.	Bar and spacing	Minimum embedment d, in.	Minimum lap splice	UHPC depth e
1	55	1152	7.9	7.5	Two rows of no. 6 at 8 in.	6	4.5	5.75
7	100	3002	16.8	12.5	Two rows of no. 6 at 3 in.	6	4.5	6
19	200	8368	20.6	14.0	Two rows of no. 8 at 4 in.	10	7.5	6.5
20	200	10,883	26.8	14.0	Two rows of no. 8 at 4 in.	10	7.5	6.5

Note: A_s = area of steel; $-M_u$ = ultimate negative bending moment. No. 6 = 19M; no. 8 = 25M; 1 in. = 25.4 mm; 1 ft = 0.305 m; 1 kip-ft = 1.356 kN-m.

Table 3 provides the reinforcement details for the negative moment region of the continuity connection. The details for the reinforcement (cover, embedment, and lap splice) are based on Graybeal.[8] The recommendations from this reference assume straight bars that are no. 8 (25M) or smaller with a yield strength not greater than 75 ksi (520 MPa) and field-cast

UHPC with a steel fiber content of 2% by volume. The spacing of the bars is based on the need to meet the maximum negative moment requirements. The diaphragm width ensures that the lap splice is sufficient for the minimum embedment. Transverse clear spacing of the lap splices shall not exceed the lap splice lengths. **Figure 2** shows the continuity joint detail.

Stage 2

Stage 2 of the analytical work involved detailed modeling of the bridges designed in stage 1. Commercial FEM analysis software was used to generate the models. These models consisted of only three girders but included details of the longitudinal joints, such as geometry and reinforcement within the joint. The primary purpose of this stage of the modeling was to assess the performance of the longitudinal joint under live load and temperature-generated effects. **Figure 3** shows the cross section and longitudinal joint detail for PCEF-39 section used in cases 1 through 6. The PCEF-47 and PCEF-63 sections are similar and only differ by taller webs. The WSDOT 103 used in cases 19 through 27 uses a 6 in. (150 mm) flange at the tips, a 6.125 in. (155.6 mm) web, and a bottom flange

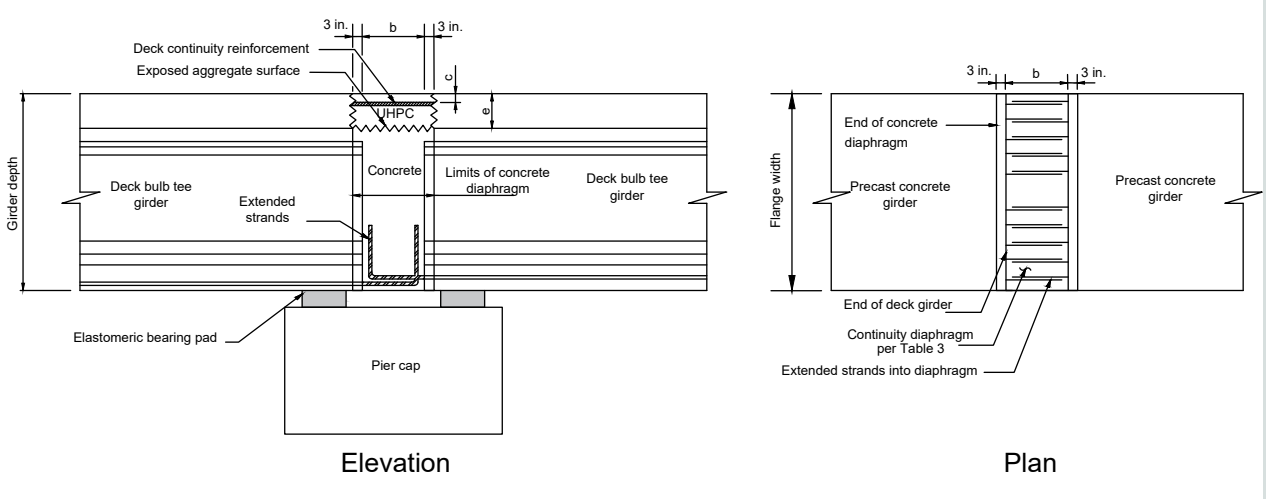

Figure 2. Continuity connection detail. Note: *b* = diaphragm width; *c* = clear cover; *e* = UHPC depth; UHPC = ultra-high-performance concrete. 1 in. = 25.4 mm.

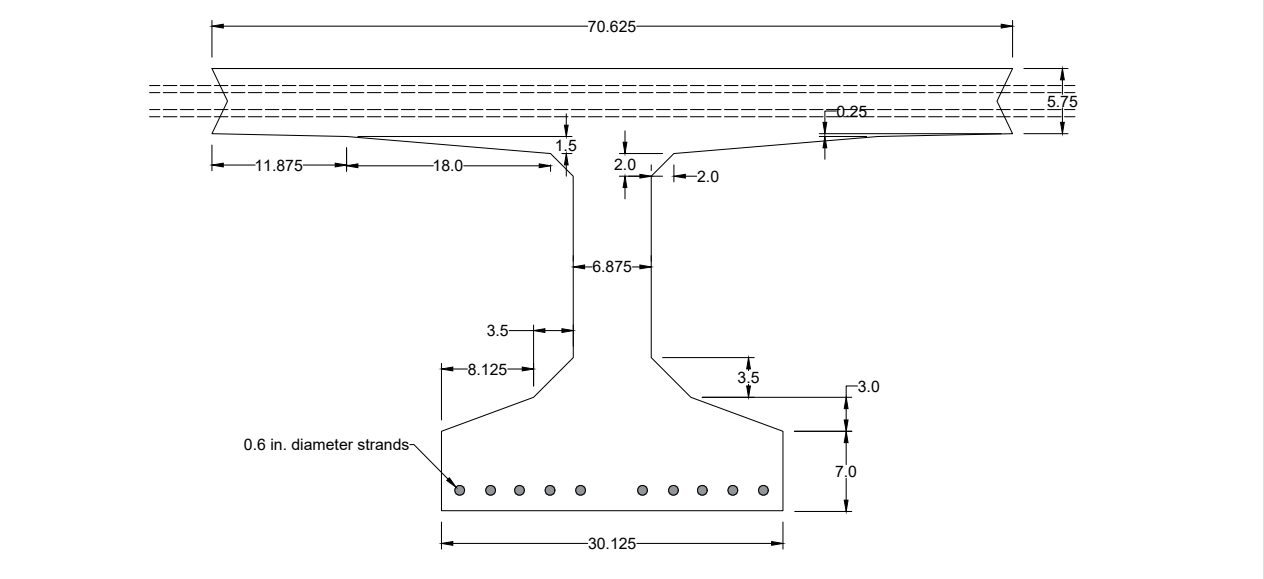

Figure 3. Precast concrete economical fabrication 39 cross section and longitudinal joint reinforcement detail. Note: all measurements are in inches. 1 in. = 25.4 mm.

width of 38.375 in. (974.73 mm). Material properties used in stage 2 modeling were consistent with materials used in stage 1 modeling (**Table 4**). Because under service loads the bridge remains completely elastic, all material used in the FEM analysis was modeled as linear elastic under both compression and tension.

The interface behavior between the UHPC within the longitudinal joint and the flanges of the high-strength prestressed concrete decked bulb tees was investigated using a tied constraint and a cohesive constraint. In a tied constraint, the surfaces of the deck bulb-tee flange and UHPC joint were tied together as both members were casted monolithically. In this constraint, the translational and rotational motion would be equal at both surfaces. This allows for transfer of loading and reduces computation time in the model; however, it does not allow for separation at the interface, which would simulate cracking. The surface behavior based on cohesive constraint (traction-separation behavior) allows for separation to occur at the interface and simulate cracking. Modeling of the cohesive behavior requires information related to shear and tensile bond behavior between the materials. A model developed by Semendary et al.[9] for the cohesive behavior of the UHPC and high-strength concrete with exposed aggregate was used to model the interaction between the longitudinal joints and the girder surface. The damage model in the FEM software requires the peak stresses and initial stiffness values *K* for both the tensile and shear cohesive behaviors. The cohesive energy is the area under the stress displacement cohesive curves. The total energy from both the tension and shear behaviors and the portion of the total from tension and shear are also required. The properties used for the cohesive interface modeling between the UHPC and girder flanges were adopted from Semendary et al.[9]

Longitudinal versus transverse behavior Often modeling is done on reduced sections to save computational time and expense. For the longitudinal joints, the transverse behavior of the flanges is critical, and the longitudinal behavior is often ignored. This results in a slab type reduced model where only the flanges of the adjacent girders are modeled as simply supported over the webs. The problem with these reduced models is that the longitudinal behavior of the girders is often overlooked in whole or in part. Therefore, for the purpose of this analysis, full models that included three girders and two longitudinal joints were generated for all cases designed in stage 1.

The loading applied in the models consisted of a single 16 kip (71 kN) wheel load applied over a contact area of approximately 10 by 20 in. (250 by 510 mm). The load was placed at the midspan of the models and at the edge of the longitudinal joint face to create a worst case for the longitudinal joint. **Figure 4** shows the deflection of the bridge model for case 1, in which both longitudinal deflection and transverse deflection of the girders are evident. The longitudinal bending behavior created compressive strains and stresses in the top flanges and the UHPC longitudinal joints. These compressive strains caused expansion in the transverse direction from Poisson's effect. The transverse expansion was resisted by the longitudinal joints and the transversely expanding adjacent girder flanges. This caused compression in the transverse direction that reduced tensile strains and stresses from flexure in the transverse direction; however, the net stress remained tensile. In addition, localized dishing at the concentrated wheel load caused longitudinal stresses and strains in the UHPC longitudinal joint.

Table 5 shows the maximum tensile stresses for tied and cohesive interactions for all cases. The tied interaction represents a perfect bond where no slip is allowed at the interface. This would result in higher stresses in the grout and less force transfer to the dowel bars. On the other hand, the cohesive interface is a more realistic representation of the interaction between the girder and longitudinal joints. It would allow for interface separation once the maximum shear or tensile stress criterion is breached, after which the interface stresses would plateau and forces would transfer to embedded reinforcement. From here on, only cohesive interaction is considered for all of the analyses.

As shown by the tied model results, the transverse stress in the UHPC joint was typically higher than the longitudinal stress, with stresses approaching 0.25 ksi (1.7 MPa). The longitudinal stresses in the joint were typically less than 0.1 ksi (0.7 MPa) except for wider-flanged deck bulb-tee

Table 4. Stage 2 material properties

Element	Strength, ksi	Poisson's ratio μ	*E*, ksi	Coefficient of thermal expansion α, /°F
Girder normalweight concrete	f'_c = 10	0.20	6164	6.0E-06
Girder lightweight concrete	f'_c = 10	0.20	3393	6.0E-06
Ultra-high-performance concrete	f'_c = 22	0.18	8520	9.4E-06
Strands	f_u = 270	0.30	28,500	7.0E-06
Reinforcement	f_y = 60	0.27	29,000	7.0E-06

Note: *E* = elastic modulus; f'_c = compressive strength of concrete; f_u = ultimate tensile strength; f_y = yield strength. 1 ksi = 6.895 MPa; °F = (°C × 1.8) + 32.

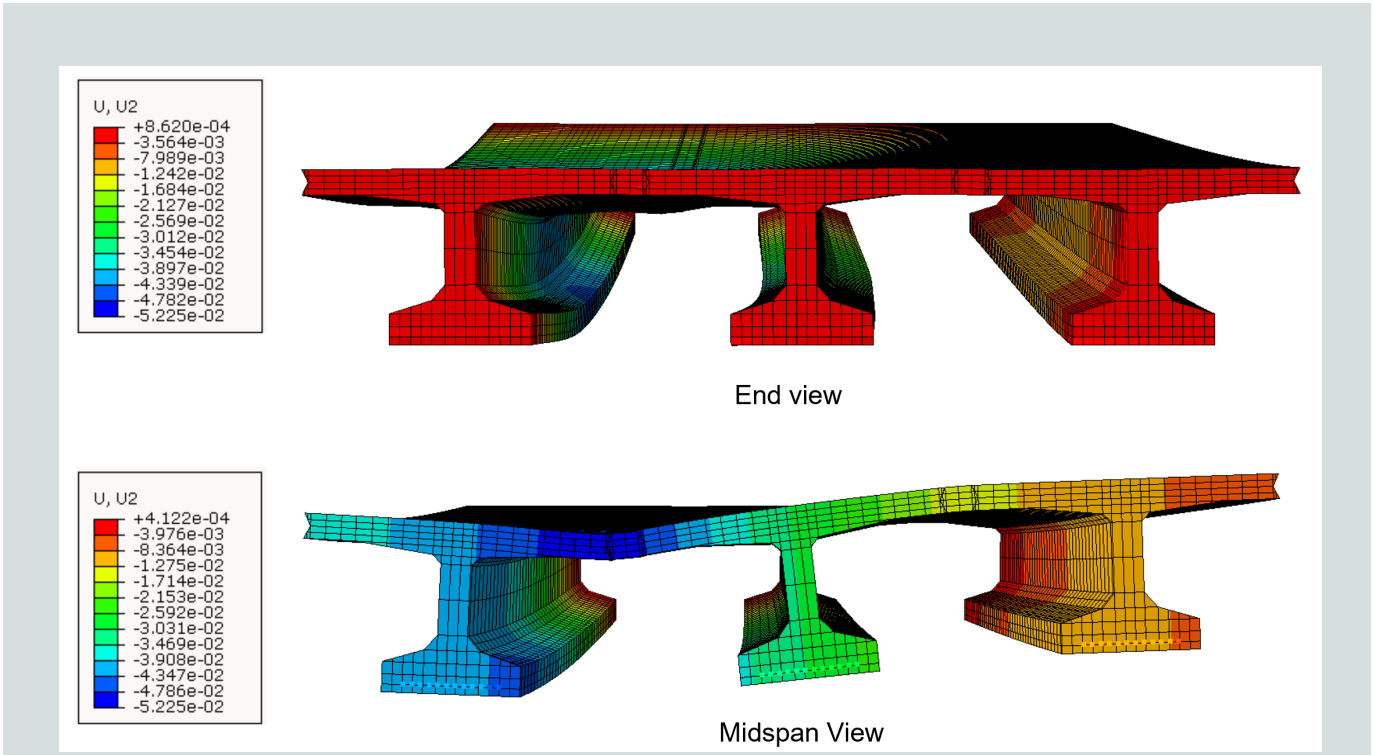

Figure 4. Deflection (in inches) of deck bulb-tee girder system under live load. Note: 1 in. = 25.4 mm.

sections. The stresses in the dowel bars were minor compared with their yield strength of 60 ksi (414 MPa). For the models with the cohesive interface, the transverse stresses in joints were lower compared with transverse stresses for the tied interface. In addition, the dowels were stressed higher compared with the tied models. This indicates stress transfer to dowel bars once the maximum stress criterion was reached at the interface, which is expected for a cohesive model. The largest longitudinal tensile stress in the joint (0.152 ksi [1.05 MPa]) occurred in case 26 for the 96 in. (2.4 m) flange lightweight concrete WSDOT section. Nearly all transverse tensile stresses in the joints were less than 0.1 ksi, with the largest (0.0921 ksi [0.635 MPa]) occurring in case 10 for the 70.625 in. (1.7939 m) flange precast concrete economical fabrication section that was 47 in. (1.2 m) deep.

Figure 5 shows the stresses for the cohesive model of case 1 at midspan. As expected, in the longitudinal direction the bottoms of the girders experienced tension and the top flanges were subjected to compression. The right edge of the far-right girder had compression in the top of the flange and tension on the bottom of the flange from the loading occurring at this location. In the transverse direction, the flanges near the loading experienced compression on the top and tension on the bottom. The top of the flanges near the web/flange junction experienced high tension.

Skew For modeling the skewed ends, the reinforcement doweled into the joint from the flanges was fanned to allow for placement without interference. Because skew is critical for short-span bridges, only cases 1, 2, and 3 (having a span of 55 ft [17 m] and skew of 0, 15, and 30 degrees, respectively) were investigated. Cohesive interaction between the girder and the UHPC was considered. A 16 kip (71 kN) live load was placed near the end of the models, close to the longitudinal joint, to evaluate the effect of skew on the longitudinal joint. The placement of the load near the end of the span increased the maximum transverse stress in the joint by 24% and 18% for 15-degree and 30-degree skew, respectively, compared with loading at midspan. For models without skew, the increase in stress was only 5%. The maximum longitudinal stress in the joint increased by 43% and 17% for 15-degree and 30-degree skew, respectively, but decreased by 5% for the model without skew. The 15-degree model showed an increase in stresses in the joint in both the transverse and longitudinal directions compared with the nonskewed model. The 30-degree skewed model had lower stresses compared with the 15-degree model. The 30-degree model also had lower transverse joint and dowel bar stresses compared with the nonskewed model but higher longitudinal joint stress. The higher joint stresses in skewed models compared with nonskewed models can be attributed to differences in the reinforcement placement at the ends due to the skew to avoid interference. There are also differences in how load gets transferred with skew and nonskew profiles. Higher joint stresses in skewed models highlight the importance of skew consideration in longitudinal joint detailing. Therefore, it is suggested that a skewed bridge profile be considered for the experimental testing. The stress in the dowels decreased for all models loaded near the support compared with midspan loading. In addition, there was no clear effect from the skew for the models.

Table 5. Stress comparison for tied versus cohesive interface

Case	Maximum tensile stress, ksi (tied models)			Maximum tensile stress, ksi (cohesion models)		
	Shear key		Dowels	Shear key		Dowels
	Longitudinal	Transverse		Longitudinal	Transverse	
1	0.1034	0.2152	0.45	0.0930	0.0505	4.44
2	0.1158	0.2333	0.44	0.0868	0.0456	5.46
3	0.0906	0.2088	0.41	0.0957	0.0368	3.02
4	0.0890	0.1979	0.41	0.0622	0.0628	4.28
5	0.0809	0.1969	0.68	0.0725	0.0342	3.83
6	0.1087	0.1816	0.96	0.1157	0.0184	3.66
7	0.0729	0.2256	0.44	0.1007	0.0599	2.84
8	0.0799	0.2110	0.96	0.0771	0.0271	6.17
9	0.0474	0.1662	0.88	0.0337	0.0140	5.52
10	0.0839	0.2422	0.84	0.0622	0.0921	6.58
11	0.0502	0.1679	0.88	0.0144	0.0189	5.68
12	0.0792	0.1930	0.89	0.0571	0.0103	6.20
13	0.1013	0.2489	1.04	0.1351	0.0335	5.48
14	0.0956	0.2107	1.02	0.0871	0.0180	5.82
15	0.0728	0.0169	5.29	0.0728	0.0169	5.29
16	0.0850	0.2314	0.98	0.0596	0.0396	5.85
17	0.0729	0.1829	0.62	0.0342	0.0148	5.40
18	0.0780	0.1874	0.91	0.0412	0.0082	5.75
19	0.0506	0.1849	0.30	0.0215	0.0188	4.40
20	0.1349	0.2574	0.51	0.0966	0.0295	6.35
21	0.0836	0.2541	0.52	0.0516	0.0217	5.43
22	0.0584	0.1985	0.20	0.0108	0.0736	4.95
23	0.0432	0.1739	0.52	0.0212	0.0233	5.20
24	0.0137	0.1732	0.63	0.0108	0.0171	4.84
25	0.1063	0.2616	0.84	0.0804	0.0292	6.59
26	0.1786	0.2463	0.91	0.1522	0.0333	7.51
27	0.0540	0.1877	0.29	0.0108	0.0880	5.87

Note: 1 ksi = 6.895 MPa.

Lightweight versus normalweight concrete Lightweight concrete was used in the 200 ft (61 m) spans with the WSDOT 103 in. (2.62 m) deep sections to compare the effects with the normalweight concrete. The lightweight concrete was used in this large section because it would likely require lightweight concrete for shipping purposes. The use of lightweight concrete increased stresses in the longitudinal joint in both directions and in the dowel bars for all cases with the one exception of the longitudinal stress for the 96 in. (2.4 m) flange with no skew. The increase in stresses in the longitudinal joint is likely due to the lower assumed stiffness of the girders when using lightweight concrete compared with normalweight concrete. This would lead to more force being transferred to stiffer sections, such as the UHPC longitudinal joint. The literature does not contain information on the bond characteristics between exposed-aggregate lightweight

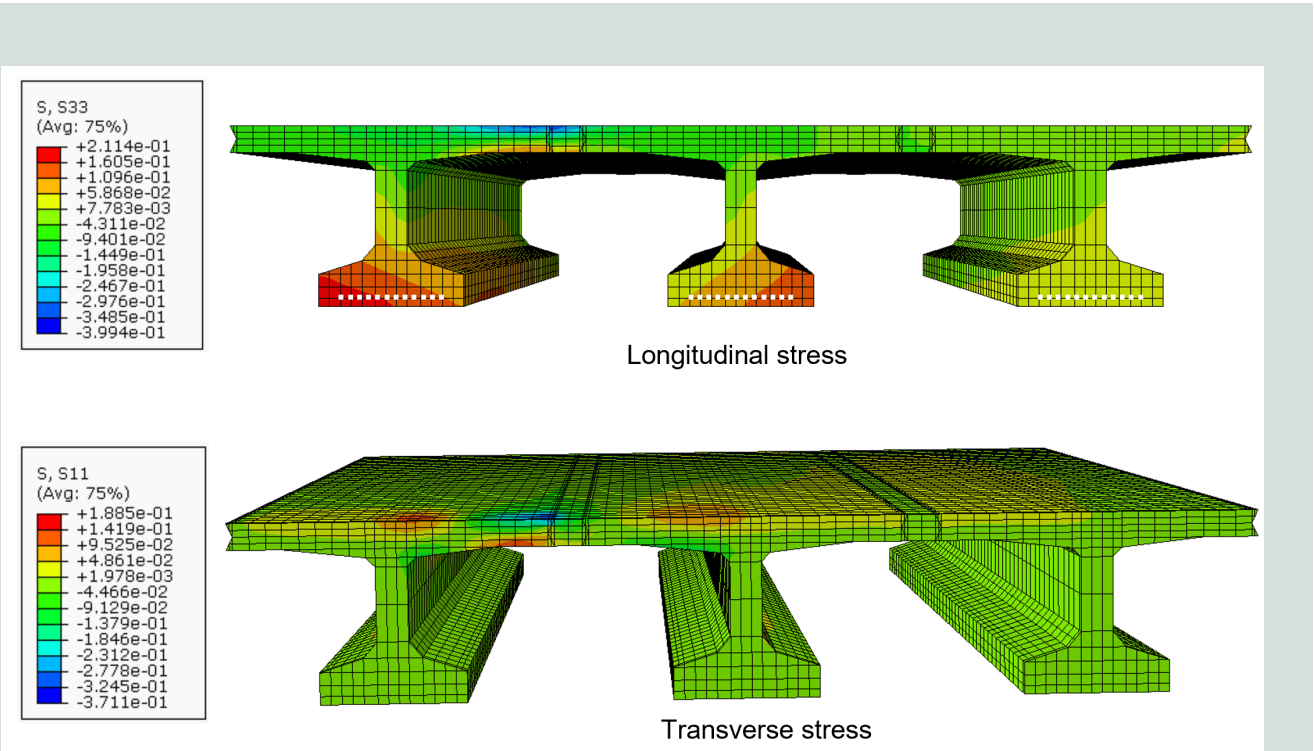

Figure 5. Stresses (in ksi) at midspan for case 1 under live loading (cohesive model). Note: 1 ksi = 6.895 MPa.

concrete finishes and UHPC. Some work has been performed on UHPC and lightweight concrete, but this was for connections with different geometries.[10] Therefore, the models used assumed parameters that were the same as with the normal high-strength concrete.

Temperature The AASHTO LRFD specifications account for uniform temperature change in a bridge by one of two procedures. Procedure A or B can be used for bridges with concrete decks having concrete or steel girders. Procedure A involves a specified maximum and minimum extended temperature based on material and a climate condition of moderate or cold. The thermal deformation effects are based on the difference of the specified maximum or minimum temperature and the base construction temperature assumed in design. Procedure B involves taking the difference in maximum and minimum temperatures determined from contour figures in the AASHTO LRFD specifications. The maximum and minimum temperatures determined from procedure A or B are then used to determine the design thermal movement range Δ_T (AASHTO LRFD specifications article 3.12.2.3).

In addition to the uniform temperature change, the AASHTO LRFD specifications also specify a thermal gradient through the depth of the bridge. The thermal gradient is dependent on the zone location of the bridge, the depth of the bridge, and the material type. Both positive and negative temperature gradients should be considered.

Both the uniform and thermal gradient temperature effects are thought of in terms of expansion and contraction of the bridge and the associated forces and stresses that may be generated if restraint resists the movements; however, temperatures can also change during construction of the bridge and affect connections such as the longitudinal joint in the deck bulb-tee bridges.

Increases in temperature after bridge completion cause longitudinal and transverse expansion of the girders. The transverse expansion is resisted by adjoining girders and the longitudinal joint expansion. This creates compression in the longitudinal joints; however, if the expansion of the girders occurs during construction, before the longitudinal joint is cast and cured, subsequent cooling of the joints and girders can create detrimental tensile strains and stresses in the joint. Therefore, analyses were performed assuming a uniform temperature drop of 80°F (27°C) (procedure A for cold regions).

The FEM software analyzed the temperature in four steps. In the first step, only deck bulb-tee girders were active, with the shear keys deactivated using the model change operation in the software. In the next step, the temperature load was applied using the predefined field option. In the following step, the shear keys were turned on to imitate grouting. Finally, the temperature gradient was gradually removed to simulate the cooling of the girder system. Table 4 shows the thermal properties of the model components.

Table 6 provides the results of the uniform temperature analyses using the cohesive models. The stresses are higher than the live load stresses (Table 5). Longitudinal stresses in the

Table 6. Maximum tensile stresses for uniform temperature and gradient temperature loadings

Case	Maximum tensile stress, ksi (uniform temperature)			Maximum tensile stress, ksi (temperature gradient)		
	Shear key		Dowels	Shear key		Dowels
	Longitudinal	Transverse		Longitudinal	Transverse	
1	2.165	0.0848	11.40	2.075	0.2366	10.39
2	2.176	0.4027	18.30	2.109	0.2473	10.59
3	2.030	0.3359	47.22	2.068	0.2538	25.04
4	2.166	0.1572	10.57	n/a	n/a	n/a
5	2.055	0.3759	41.14	2.610	0.1984	16.28
6	2.194	0.2482	2.50	n/a	n/a	n/a
7	1.864	0.7057	7.15	1.897	0.3237	2.98
8	2.179	0.2365	14.92	2.015	0.2170	9.11
9	2.195	0.3598	18.85	1.684	0.4378	7.61
10	1.997	0.1678	10.87	n/a	n/a	n/a
11	2.162	0.3391	16.19	2.534	0.6074	9.55
12	2.175	0.1206	6.27	n/a	n/a	n/a
13	1.774	0.3619	4.94	1.737	0.3737	4.17
14	2.172	0.2509	12.02	1.976	0.1704	7.55
15	2.196	0.2782	12.18	1.982	0.1605	6.43
16	2.170	0.2167	3.68	n/a	n/a	n/a
17	2.191	0.3132	17.09	2.734	0.1583	7.31
18	1.720	0.0499	6.03	n/a	n/a	n/a
19	2.202	0.3570	5.76	2.478	0.2194	11.37
20	2.241	0.3567	5.21	n/a	n/a	n/a
21	2.233	0.2900	8.71	n/a	n/a	n/a
22	2.202	0.3370	5.02	n/a	n/a	n/a
23	2.093	0.3401	5.54	n/a	n/a	n/a
24	2.754	0.2198	7.73	n/a	n/a	n/a
25	2.150	0.2642	7.63	n/a	n/a	n/a
26	2.157	0.3459	4.84	n/a	n/a	n/a
27	2.091	0.3383	4.91	n/a	n/a	n/a

Note: 1 ksi = 6.895 MPa; n/a = model not run for this case.

joint were higher than the transverse stresses. This is likely due to the higher coefficient of thermal expansion used for the UHPC relative to the girders. The stresses in the dowel bars were high, especially for the models with skews. High stresses were obtained in the dowel bars for the highly skewed short span (cases 3 and 5).

The traction-separation failure model was used to determine cracking. Equation (1) defines the failure model.[9] Values greater than 1.0 indicate a crack.

$$\left(\frac{\sigma_n}{\sigma_{allow}}\right)^2+\left(\frac{\tau_1}{\tau_{allow}}\right)^2+\left(\frac{\tau_2}{\tau_{allow}}\right)^2\geq 1.0 \quad (1)$$

where

σ_n = normal stress

σ_{allow} = allowable normal stress taken from literature/research

τ_1 = shear stress in direction 1

τ_{allow} = allowable shear stress taken from literature/research

τ_2 = shear stress in direction 2

Figure 6 shows the traction-separation failure model results for the interface of case 3 subjected to the uniform temperature change. The results are highest near the end of the joint. The maximum value is approximately 0.5, which does not indicate cracking.

In addition, a temperature gradient can occur in the girders prior to longitudinal-joint UHPC placement and curing. Therefore, a drop in a temperature gradient approximately equal to the AASHTO LRFD specifications' temperature gradient for zone 1 was applied in models to determine effects on the longitudinal joint. The gradient was approximated by a fourth-order polynomial equation to allow more-direct input into the software. Some of the models were investigated using the temperature gradient (Table 6). The maximum tensile stresses developed from the temperature gradient were similar to the uniform temperature results. The stresses were higher for skewed models and much more significant than live load stresses.

Stage 3

The primary objective of this stage of modeling was to evaluate the live load distribution factors for bridges with longitudinal UHPC joints. Five bridge models (corresponding to cases 1, 7, 13, 19, and 20) with five girders each were prepared such that the joints between girders were modeled as UHPC with cohesive interface between girder and the UHPC. These bridges had a minimum width exceeding 31 ft (9.4 m) to allow for at least two lanes. The bridge models were analyzed under AASHTO LRFD specifications HL-93 load.

Moment LLDFs have been determined using a variety of methods over the years. Ghosn et al.[11] assumed each LLDF for a girder was equal to the ratio of the static strain in the girder over the total of the strains on all the girders. Stallings and Yoo[12] used weighting factors to account for differences in the section modulus of exterior girders with interior girders. Because the girders in the models used for this research had the same section modulus for exterior and interior girders, the weighting factors were set equal to 1. In addition, the modulus of elasticity was same for each girder. Therefore, the LLDF was determined by dividing the stress in each deck bulb-tee girder from the analysis by the sum of all of the girder stresses (Eq. [2]).

$$LLDF_i = \frac{\varepsilon_i w_i}{\sum_1^k \varepsilon_i w_i} = \frac{\sigma_i}{\sum_1^k \sigma_i} \quad (2)$$

where

$LLDF_i$ = moment LLDF for girder i

ε_i = static strain in girder i

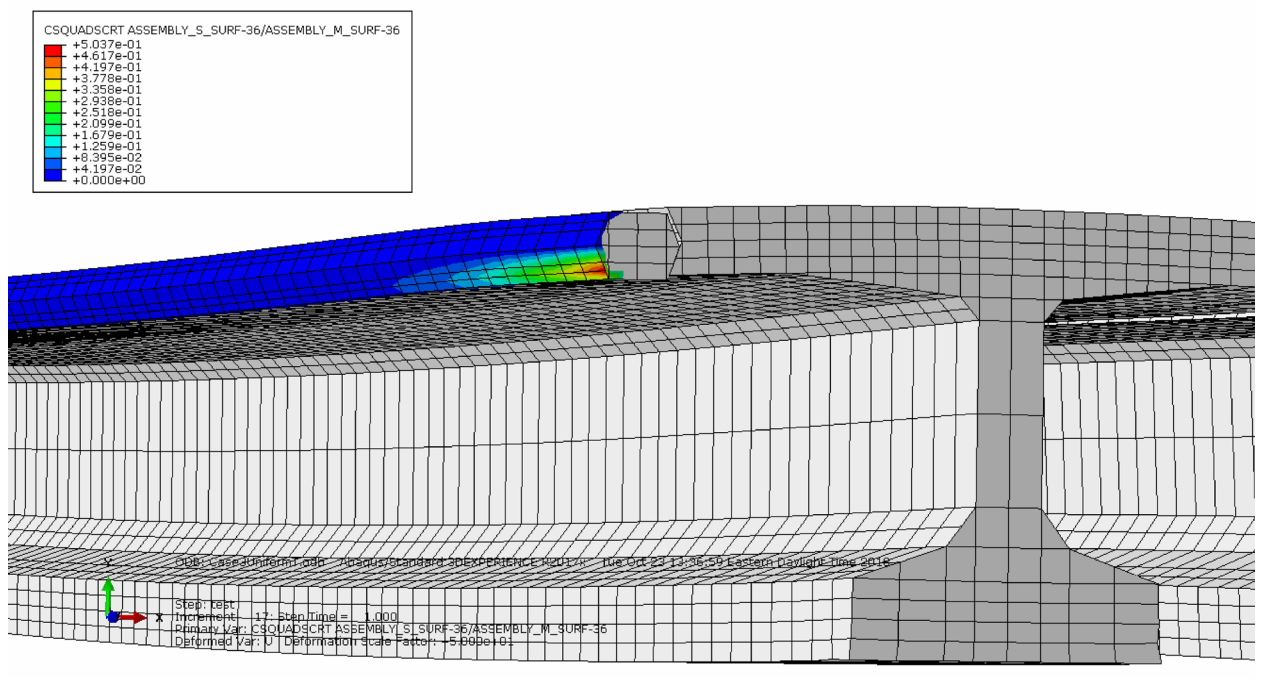

Figure 6. Traction-separation results for case 3 under uniform temperature.

w_i = ratio of section modulus for girder i to interior girder

k = number of girders in the bridge

σ_i = stress in girder i from live loading

For moment distribution factors, the loading was positioned on the bridge to create the maximum moment along the span and to produce the largest effect for the distribution factors. **Figure 7** shows the longitudinal and lateral positioning of the loading on bridge deck in the top and middle images, respectively. The bottom image of Fig. 10 shows the longitudinal stresses at midspan for case 1 under the HL-93 loading. **Table 7** shows the LLDF for moment in the interior and exterior girders under single- and double-lane loading, along with the design moment LLDF calculated using the AASHTO LRFD specifications' formula. The moment LLDFs from the FEM analyses are lower than those determined by the AASHTO LRFD specifications' formula for the exterior girders. For the interior girders, the moment LLDFs from the FEM analyses are comparable and conservative based on the AASHTO LRFD specifications' formula except for case 19, which had a large span and closely spaced girders.

To determine the distribution factors for shear, the truck loading was moved longitudinally to the support. The shear in each girder was then divided by the total shear for the end of the bridge to determine the LLDFs for shear. The LLDFs for the shear at the end that was loaded are more critical (Table 7), and the shear FEM analyses are lower than those determined by the AASHTO LRFD specifications' formula for the interior girders. However, for the exterior girders, the FEM analyses showed higher shear LLDF than the AASHTO LRFD specifications' formula.

Conclusion

Based on the analytical program, the following observations and general conclusions were drawn:

- The usage of UHPC in continuity connections between spans of deck bulb tees can reduce the length of the connection due to the bond strength of UHPC.

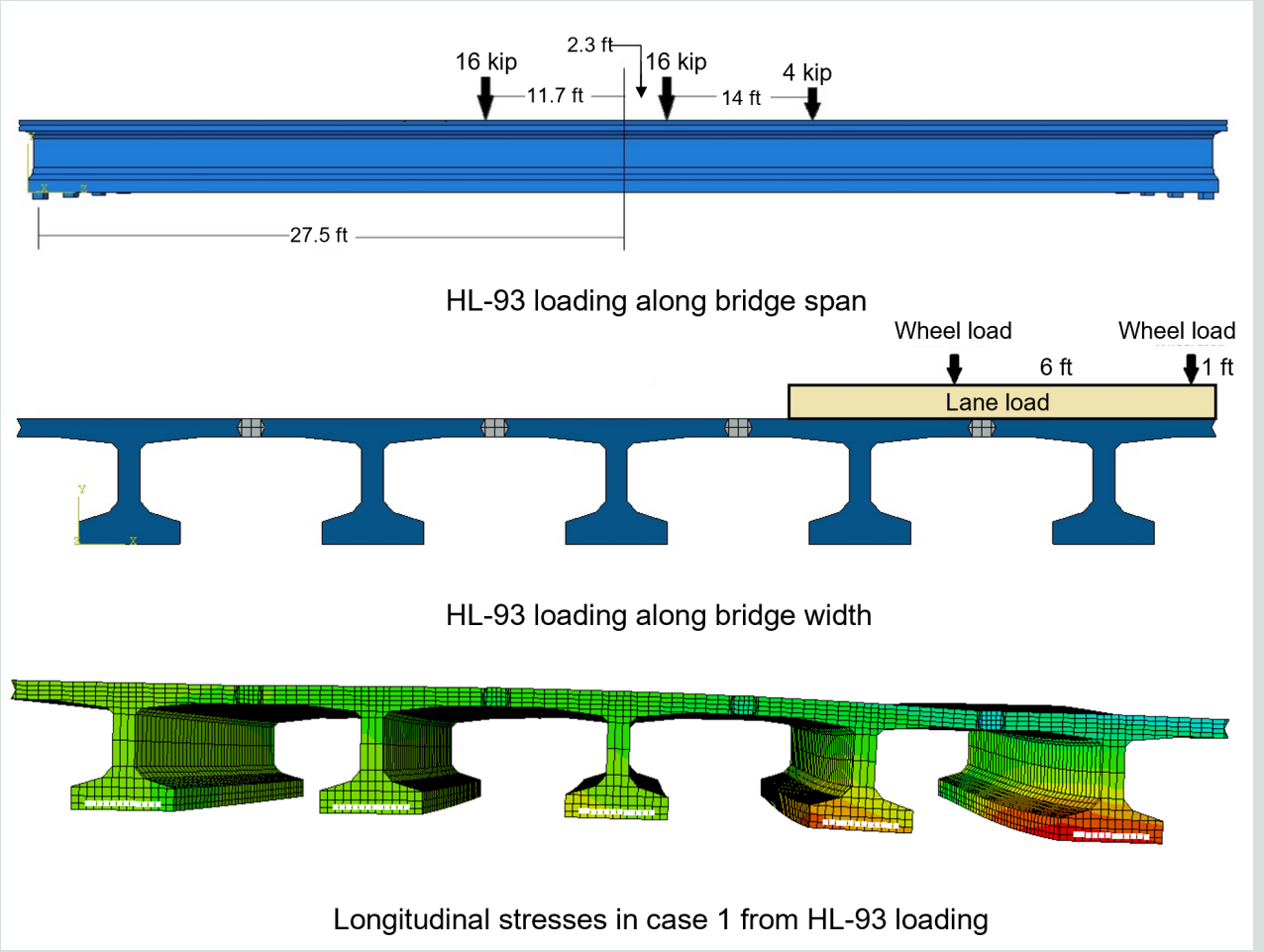

Figure 7. HL-93 loading placement and longitudinal stresses generated for case 1. Note: 1 ft = 0.305 m; 1 kip = 4.448 kN.

Table 7. Comparison of LLDF from finite element modeling analysis and AASHTO LRFD specifications formula

LLDF type	Case	Finite element modeling moment LLDF				AASHTO LRFD specifications design moment LLDF	
		Interior girder		Exterior girder		Interior girder	Exterior girder
		One lane loaded	Two lanes loaded	Two lanes loaded	One lane loaded		
Moment LLDF	1	0.364	0.515	0.591	0.522	0.656	0.813
	7	0.328	0.483	0.516	0.521	0.580	0.814
	13	0.320	0.518	0.456	0.559	0.555	0.814
	19	0.389	0.661	0.530	0.560	0.569	0.814
	20	0.315	0.578	0.614	0.637	0.696	1.059
Shear LLDF	1	0.378	0.512	0.936	0.568	0.698	0.813
	7	0.350	0.519	0.942	0.659	0.699	0.814
	13	0.351	0.513	0.887	0.667	0.699	0.814
	19	0.372	0.432	0.787	0.555	0.699	0.814
	20	0.178	0.714	1.138	0.889	0.849	1.059

Note: LLDF = live-load moment distribution factor.

- Longitudinal bending behavior from live loading of deck bulb-tee bridges creates compressive strains and stresses in the top flanges and the UHPC longitudinal joints. These compressive strains cause expansion in the transverse direction from Poisson's effect. The transverse expansion is resisted by the longitudinal joint and the transversely expanding adjacent girder flanges. This causes compression in the transverse direction that reduces tensile strains and stresses from flexure in the transverse direction, but the net stress remains tensile. In addition, localized dishing at the concentrated wheel load causes longitudinal stresses and strains in the UHPC longitudinal joint. Stresses from live loading are not significant.

- Both uniform and gradient temperature effects can change during construction of the bridge and affect connections such as the longitudinal joint in the deck bulb-tee bridges. If thermal expansion of the girders occurs during construction before the longitudinal joints are cast and cured, subsequent cooling of the joints and girders can create detrimental tensile strains and stresses in the joint. The analyses of a uniform temperature drop of 80°F (27°C) (procedure A for cold regions) resulted in stresses much higher than the live loading conditions investigated. Longitudinal stresses in the joint were higher than the transverse stresses. This was due to the larger coefficient of thermal expansion for the UHPC relative to the girders. High stresses were also determined in the dowel bars for the highly skewed short spans.

- A large uniform temperature change is less likely to occur during construction compared with a temperature gradient. Analyses from a gradient temperature drop equivalent to AASHTO LRFD specifications Zone 1 resulted in stresses much higher than the live loading conditions investigated. Longitudinal stresses in the joint were higher than the transverse stresses. This was due to the larger coefficient of thermal expansion for the UHPC relative to the girders. High stresses were also determined in the dowel bars for the highly skewed short spans.

- The analytical results showed that the moment LLDFs were lower than those determined by the AASHTO LRFD specifications for the exterior girders. For the interior girders, the moment LLDFs from the analyses were comparable and conservative based on the AASHTO LRFD specifications except for a large span and closely spaced girder bridge (case 19). The LLDFs for shear from the analyses are lower than those determined by the AASHTO LRFD specifications for the interior girders. However, the analyses showed higher shear LLDFs than the AASHTO LRFD specifications for the exterior girders.

Acknowledgments

The research presented in this paper was a part of National Cooperative Highway Research Program (NCHRP) Project 18-18, which was documented in Steinberg et al.[13] The authors wish to thank the NCHRP Project Panel and the senior program officers, Ahmad Abu-Hawash and Waseem Dekelbab, for their project oversight and valuable insight and feedback throughout the project. The material present-

ed in this paper is reproduced with permission from the Transportation Research Board.

References

1. Stanton, J. F., and A. H. Mattock. 1987. "Load Distribution and Connection Design for Precast Stemmed Multibeam Bridge Superstructures." NCHRP (National Cooperative Highway Research Program) report 287. Washington, DC: Transportation Research Board.

2. Baer, Clark. 2013. "Investigation of Longitudinal Joints Between Precast Prestressed Deck Bulb Tee Girders Using Latex Modified Concrete." MS thesis, University of South Carolina.

3. Chapman, Cheryl Elizabeth. 2010. "Behavior of Precast Bridge Deck Joints with Small Bend Diameter U-Bars." MS thesis, University of Tennessee–Knoxville.

4. Li, L., Z. J. Ma, M. Griffey, and R. Oesterle. 2010. "Improved Longitudinal Joint Details in Decked Bulb Tees for Accelerated Bridge Construction: Concept Development." *ASCE Journal of Bridge Engineering* 15 (3): 327–336.

5. French, C., C. Shield, D. Klaseus, M. Smith, W. Eriksson, Z. Ma, P. Zhu, S. Lewis, and C. Chapman. 2011. "Cast-in-Place Concrete Connections for Precast Deck Systems." NCHRP web-only document 173. https://doi.org/10.17226/17643.

6. Seibert, Peter J., V. H. Perry, and D. Corvez. 2021. "Performance Evaluation of Field Cast UHPC Connections for Precast Bridge Elements." *International Interactive Symposium on Ultra-High Performance Concrete* 2 (1). https://doi.org/10.21838/uhpc.9634.

7. AASHTO (American Association of State Highway and Transportation Officials). 2020. *AASHTO LRFD Bridge Design Specifications*. 9th ed. Washington, DC: AASHTO.

8. Graybeal, B. 2014. "Design and Construction of Field-Cast UHPC Connections." FHWA-HRT-14-084. https://www.fhwa.dot.gov/publications/research/infrastructure/structures/14084/14084.pdf.

9. Semendary, A. A., W. K. Hamid, E. P. Steinberg, and I. Khoury. 2020. "Shear Friction Performance between High Strength Concrete (HSC) and Ultra High Performance Concrete (UHPC) for Bridge Connection Applications." *Engineering Structures*, no. 205: 110122. https://doi.org/10.1016/J.ENGSTRUCT.2019.110122.

10. Banta, T. 2005. "Horizontal Shear Transfer Between Ultra High Performance Concrete and Lightweight Concrete." MS thesis, Virginia Polytechnic and State University.

11. Ghosn, M., F. Moses, and J. Gobieski. 1986. "Evaluation of Steel Bridges Using In-Service Testing." In *Structural Design of Bridges*, ed. Elizabeth W. Kaplan, 71–78. Washington, DC: Transportation Research Record.

12. Stallings, J. M., and C. H. Yoo. 1993. "Tests and Ratings of Short-Span Steel Bridges." *Journal of Structural Engineering* 119 (7): 2150–68. https://doi.org/10.1061/(ASCE)0733-9445(1993)119:7(2150).

13. Steinberg, E., K. Walsh, W. Hamid, A. Chlosta, C. Slyh, R. Miller, B. Shahrooz, A. Haroon, R. Castrodale, and C. Prussack. 2022. "Design and Construction of Deck Bulb Tee Girder Bridges with UHPC Connections." National Cooperative Highway Research Program Research Report 999. Washington, DC: The National Academies Press. https://doi.org/10.17226/26644.

Notation

A_s = area of steel

b = diaphragm width

d = minimum embedment

e = ultra-high-performance concrete depth

E = modulus of elasticity

f'_c = compressive strength of concrete

f_u = ultimate tensile strength

f_y = yield strength

k = number of girders in the bridge

K = initial stiffness

l_d = development length

l_s = lap splice length

$LLDF_i$ = live load moment distribution factor for girder i

$-M_u$ = ultimate negative bending moment

V = shear force

w_i = ratio of section modulus for girder i to interior girder

α = coefficient of thermal expansion

δ_f = final displacement

Δ_T = design thermal movement range

ε_i = static strain in girder *i*

μ = Poisson's ratio

σ_{allow} = allowable normal stress taken from literature/research

σ_i = stress in girder *i* from live loading

σ_{max} = tensile bond strength

σ_n = normal stress

τ_1 = the shear stress in direction 1

τ_2 = the shear stress in direction 2

τ_{allow} = allowable shear stress taken from literature/research

τ_{max} = shear strength

About the authors

Abdullah Haroon is a graduate research assistant in the Department of Civil and Environmental Engineering at the University of Cincinnati in Cincinnati, Ohio.

Waleed Hamid is a lecturer in the Department of Civil Engineering at the University of Fallujah in Iraq.

Eric Steinberg, PhD, PE, is a professor in the Department of Civil Engineering at Ohio University in Athens, Ohio.

Kenneth Walsh, PhD, PE, is an associate professor in the Department of Civil Engineering at Ohio University.

Richard Miller, PhD, PE, is a professor in the Department of Civil and Environmental Engineering at the University of Cincinnati.

Bahram Shahrooz, PhD, PE, is a professor in the Department of Civil and Environmental Engineering at the University of Cincinnati.

Abstract

Precast concrete deck bulb-tee girder systems offer an excellent choice for prestressed concrete bridges with spans of 100 ft (30.48 m) or more. These girders are placed side by side in the field and connected using longitudinal joints. The wide top flange of the girders acts as a deck, eliminating the need for a cast-in-place concrete deck and providing a solution for accelerated bridge construction. However, the longitudinal joints between the girders often crack under service loads, allowing for water and deicing chemicals to enter the system and cause corrosion. An analytical study with ultra-high-performance concrete (UHPC) longitudinal joints was performed to investigate the joint performance when subjected to thermal and live loads. A continuity diaphragm with UHPC in the top flange was also investigated for negative moment over pier. Results of the investigation suggest that the use of UHPC can improve the performance of the connections. The high bond strength of the UHPC reduces the connection length and allows for simpler reinforcement details.

Keywords

AASHTO, ABC, accelerated bridge construction, American Association of State Highway and Transportation Officials, bulb-tee girder, connection, girder, UHPC, ultra-high-performance concrete.

Review policy

This paper was reviewed in accordance with the Precast/Prestressed Concrete Institute's peer-review process. The Precast/Prestressed Concrete Institute is not responsible for statements made by authors of papers in *PCI Journal*. No payment is offered.

Publishing details

This paper appears in *PCI Journal* (ISSN 0887-9672) V. 68, No.3, May–June 2023, and can be found at https://doi.org/10.15554/pcij68.3-04. *PCI Journal* is published bimonthly by the Precast/Prestressed Concrete Institute, 8770 W. Bryn Mawr Ave., Suite 1150, Chicago, IL 60631.

Reader comments

Please address any reader comments to *PCI Journal* editor-in-chief Tom Klemens at tklemens@pci.org or Precast/Prestressed Concrete Institute, c/o *PCI Journal*, 8770 W. Bryn Mawr Ave., Suite 1150, Chicago, IL 60631.